Int. J. Electrochem. Sci., 7 **(2012)** 11426 - 11443

International Journal of
ELECTROCHEMICAL
SCIENCE
www.electrochemsci.org

Electrocatalytic Oxidation of Alcohols, Sulfides and Hydrogen Peroxide Based on Hybrid Composite of Ruthenium Hexacyanoferrate and Multi-Walled Carbon Nanotubes

Kuo-Chiang Lin, Chuen-Pon Hong, Shen-Ming Chen[*]

Electroanalysis and Bioelectrochemistry Lab,Department of Chemical Engineering and Biotechnology, National Taipei University of Technology, No.1, Section 3, Chung-Hsiao East Road, Taipei 106, Taiwan (ROC).
[*]E-mail: smchen78@ms15.hinet.net

Received: 21 September 2012 / *Accepted:* 11 October 2012 / *Published:* 1 November 2012

An electrochemical sensor of alcohols, sulfides, and hydrogen peroxide (H_2O_2) has been investigated with hybrid composite of ruthenium hexacyanoferrate (RuHCF) and multi-walled carbon nanotubes (MWCNT). The formed MWCNT-RuHCF composite was examined in acidic solution and found four characteristic redox couples revealed RuHCF redox process. It was stable and found higher current response when RuHCF hybrid with MWCNT. It showed good electrocatalytic oxidation to alcohols including ethanol, propanol, isopropanol, and sulfides including L-cysteine, thiosulfate, respectively. Particularly, both electrocatalytic oxidation and reduction of H_2O_2 can be performed by this composite. Applied potential at -0.1 V, it showed a linear range of $0-1.2\times10^{-4}$ M, with a detection limit of 10^{-5} M (S/N = 3) and a significant sensitivity of 123.2 μA mM^{-1} cm^{-2}. Ethanol, propanol, and isopropanol were determined at +1.05 V, +1.15 V, and +1.23 V, respectively. Linear range of $2\times10^{-4}-1.7\times10^{-3}$ M, $4\times10^{-4}-1.7\times10^{-3}$ M, and $0-8\times10^{-4}$ M were estimated for these alcohols. The sensitivity was 4548.4 μA M^{-1} cm^{-2}, 12544.6 μA M^{-1} cm^{-2}, 38543.1 μA M^{-1} cm^{-2}, with detection limit of 10^{-4} M, 10^{-5} M, and 10^{-5} M (S/N = 3), respectively.

Keywords: Ruthenium hexacyanoferrate; Multi-walled carbon nanotube; Alcohol; Sulfide; Hydrogen peroxide

1. INTRODUCTION

Polynuclear transition metal hexacyanoferrates (MeHCF) have many applications such as chemical sensors, charge storage, electroanalysis, ion exchange, electron mediator, and electrocatalysis [1–14]. They are usually formed by electrodeposition and coprecipitation method. Transition metal

hexacyanoferrates are interesting materials for charge storage due to their unique structural characteristics such as three-dimensional network and tunnel structure.

MeHCF deposits as electrode modifiers have been extensively investigated to exploit their electrocatalytic properties for the detection of various organic and inorganic species, e.g. different cations [15], glucose [16], hydrazine [17], and AA [18,19]. Mixed metal HCFs as electrode coatings have also been studied and employed in improved electrochemical sensing, for example CoCuHCF in potentiometric detection of hydrazine [20] and FeCoHCF in amperometric sensing of hydrogen peroxide [21]. Up to now, many kinds of MHCFs prepared by electrodeposition on various electrode substances has been reported, such as PdHCF [22,23], InHCF [24], VHCF [25], YHCF [26], RuHCF [27,28], CoHCF [29], NiHCF [30], ZnHCF [31,32] and BiHCF [33]. The most notable advantages of MHCF electrode coatings are certainly their electrocatalytic activity and prolonged stability. However, there was no report about the electrochemical behaviors of organic-inorganic hybrid composite of multi-walled carbon nanotubes (MWCNT) and RuHCF, even the morphological study. Although the electrochemical behaviors of MeHCFs might be similar, it is still necessary to investigate such kind of electroactive materials, since under different organic-inorganic composite formation on electrode surface as well as the electrochemical behaviors may be different.

Over the past few decades fuel cells have been the focus of interest to many researchers for converting chemical energy into electrical energy [34–38]. Among the various systems reported in literature, alkaline fuel cells involving the direct electrochemical oxidation of alcohols have been projected to be very much useful in portable devices and transport applications [39–41]. Considerable efforts have been directed towards the development of materials capable of performing electrocatalytic oxidation of alcohols. These studies were essentially focused on to bring down the large overpotential encountered in its direct electro-oxidation at most electrode surfaces and to increase the oxidation current density.

Thiol compounds are of special significance in biochemistry and environmental chemistry, and studies on these compounds provide critical insight into the proper physiological function and diagnosis of disease states [42–45]. L-Cysteine (CySH) is a sulfur-containing a-amino acid that plays an important role in biological systems because it binds in a special way and maintains the structure of proteins in the body. In addition, it may play an important role in the communication between the immune system cells [46]. Numerous research efforts have been performed for the determination of CySH [47–49]. Compared with the fluorimetric and spectroscopic detection methods, the electrochemical techniques have the inherent advantages of ease of miniaturization, high sensitivity, and relatively low cost as well as being less sensitive to matrix effects than other analytical techniques. In addition, these techniques can be easily electronically interfaced to a computer and, in most instances, do not require the derivatization process. However, electrochemical detection of CySH still remains challenging. CySH electrooxidation at the conventional solid electrodes, such as noble metals and carbon-based electrodes, is usually plagued by sluggish electron transfer kinetics. It needs a large over-potential for the electrooxidation process to occur at a desirable rate to attain reasonably good sensitivity [50]. In addition, the high over-potential needed significantly reduces the detection selectivity, especially for biological samples. On the other hand, electrooxidation of CySH on these electrodes at highly positive potentials causes surface oxide formation as well as the fouling effect. To

overcome these problems, some strategies have been developed and include application of pulse electrochemical detection [51,52], the use of mercury and diamond electrodes [48,51,52] and enzyme-based biosensors [53,54], and the design and applications of a variety of modified electrodes [48]. In the course of modified electrodes, the immobilized modifier on the electrode surface generally involves redox species that flip-flop between two redox states. CySH is then oxidized through an electrocatalytic conversion. Analysis of CySH with a physiological concentration of less than 300 lM has been improved greatly; however, the development of new modified electrodes for its determination is needed.

Hydrogen peroxide (H_2O_2) is important in many biological processes and biosensor development[55-57]. Besides, it is also an essential mediator in food, pharmaceutical, clinical, industrial and environmental analyses [59,60]. Reliable, sensitive and rapid determination of H_2O_2 is of practical importance. The recent studies demonstrated that surfactant treatment of MeHCF compounds is very effective in improving their electrochemical stability [61]. It was also reported that functional CNTs with dyes, nano-materials, or conducting polymers could lead to the formation of specific composites and enrich the application of CNTs [62–64].

In the current study, an efficient electrocatalytic transducer based on MWCNT-RuHCF was employed for the electrocatalytic reaction of alcohols (methanol, ethanol, propanol, isopropanol), sulfides (CySH, thiosulfate) and H_2O_2. The hybrid composite was characterized by cyclic voltammetry (CV) and scanning electron microscopy (SEM). The electrocatalytic properties were compared between RuHCF and MWCNT-RuHCF. According to potential setting, it was used to determine ethanol, propanol, isopropanol, and H_2O_2 by amperometry.

2. MATERIALS AND METHODS

2.1. Reagents and materials

Ruthenium(III) nitrate ($Ru(NO_3)_3$), potassium hexacyanoferrate(III) ($K_3Fe(CN)_6$), multi-walled carbon nanotube (MWCNT), potassium nitrate (KNO_3), nitric acid (HNO_3), methanol, ethanol, propanol, isopropanol, L-cysteine, sodium thiosulfate, and hydrogen peroxide (H_2O_2) were purchased from Sigma-Aldrich (USA). All other chemicals (Merck) used were of analytical grade (99%). Double-distilled deionized water was used to prepare all the solutions. A nitric buffer solution of pH 1.5 was prepared using KNO_3 (0.1 mol L^{-1}) and adjusting with HNO_3.

2.2. Apparatus

All electrochemical experiments were performed using CHI 1205a potentiostats (CH Instruments, USA). The BAS GCE (0.3 cm in diameter, exposed geometric surface area 0.07 cm^2, Bioanalytical Systems, Inc., USA) was used. A conventional three-electrode system was used which consists of an Ag/AgCl (3 M KCl) as a reference electrode, a GCE as a working electrode, and a platinum wire as a counter electrode. For the rest of the electrochemical studies, Ag/AgCl (3 M KCl)

was used as a reference. The morphological characterization of composite films was examined by scanning electron microscopy (SEM, S-3000H, Hitachi). Indium tin oxide (ITO) glass was the substrate of different films for SEM analysis. The buffer solution was entirely altered by deaerating using nitrogen gas atmosphere. The electrochemical cells were kept properly sealed to avoid the oxygen interference from the atmosphere. All electrochemical experiments were performed under anaerobic condition to avoid the voltammetric response of oxygen reduction in the system.

2.3. Preparation of RuHCF and MWCNT-RuHCF film modified electrodes

Since polynuclear mixed-valent films of ruthenium oxide/hexacyanoferrate and ruthenium hexacyanoferrate (RuHCF) can be easily prepared using repeatedly cyclic voltammetry [18]. Here a further work of the RuHCF and multi-walled carbon nanotube (MWCNT) hybrid composite is carried out and expected to enhance electrocatalytic current response for alcohols, sulfides, and H_2O_2.

As shown in Scheme 1, there are two procedures to prepare the film modified electrode. Firstly the called RuHCF film was firstly prepared on electrode surface in the nitric solution (pH 1.5) containing 5×10^{-3} M $Ru(NO_3)_3$ and 5×10^{-3} M $K_3Fe(CN)_6$. It was taken in the potential range of -0.3~+1.5 V, scan rate of 0.1 V s^{-1}, 60 scan cycles by repeatedly cyclic voltammetry. This modified electrode was further adhered with well-dispersed functionalized MWCNT [50] (1 mg ml^{-1}) and dried out in the oven at 40 ℃ for 10 minutes. Hence the called MWCNT-RuHCF composite was prepared on GCE or ITO electrode surface to study in this work.

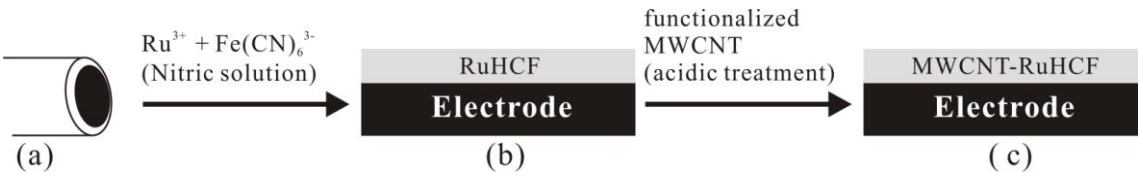

Scheme 1. Illustration of RuHCF and MWCNT-RuHCF film formation on electrode surface.

3. RESULTS AND DISCUSSION

3.1. Cyclic voltammograms of RuHCF and MWCNT-RuHCF hybrid film

The RuHCF and MWCNT hybrid composite was prepared as mentioned in section 2.3. For convenience, the hybrid composite was briefly denoted as MWCNT-RuHCF. Fig. 1A shows the voltammograms of RuHCF film growth in nitric buffer solution (pH 1.5) containing 5×10^{-3} M $Ru(NO_3)_3$ and 5×10^{-3} M $K_3Fe(CN)_6$. There are four redox couples with obvious current development in the cyclic voltammograms. The formal potential ($E^{0'}$) is found at about -0.05 V, 0.57 V, 0.87 V, and 1.07 V for redox couple 1, 2, 3, and 4, respectively. Although it is taken in more scan cycles and more higher concentration of Ru^{3+} and $Fe(CN)_6^{3-}$, it exhibits the same formal potential as our previous result [18]. And the current response is almost 5 fold than the previous result. It means that the RuHCF

formation is very stable and performed very well to contribute more current. The redox processes of four redox couples can be expressed as follows:

$$\text{Ru(II)-O/Fe(II)-CN} \rightarrow \text{Ru(III)-O/Fe(II)-CN} + e^- \quad (1)$$

$$\text{Ru(III)-O-CN-Fe(II)} \rightarrow \text{Ru(III)-O-CN-Fe(III)} + e^- \quad (2)$$

$$\text{Ru(III)-O/Fe(II)-CN} \rightarrow \text{Ru(III)-O/Fe(III)-CN} + e^- \quad (3)$$

$$\text{Ru(III)-O/Fe(III)-CN} \rightarrow \text{Ru(IV)-O/Fe(III)-CN} + e^- \quad (4)$$

Subsequently, the RuHCF/GCE or RuHCF/ITO was covered by 10 μl MWCNT drop (1 mg ml^{-1}) and dried out to form MWCNT-RuHCF/GCE or MWCNT-RuHCF/ITO for further study.

In order to confirm the RuHCF and MWCNT-RuHCF composites were successfully immobilized on the electrode surface, it was transferred to blank solution for CV studies. By the way, the influence of scan rate on the electrochemical response of RuHCF and MWCNT-RuHCF composites were investigated and compared.

Table 1. Potentials of RuHCF and MWCNT-RuHCF redox peaks related to scan rates.

Scan rate	RuHCF				MWCNT-RuHCF			
v [a]/mV s^{-1}	E_{pa1} [b]/V	E_{pc1} [c]/V	$E^{0'}{}_1$ [d]/V	ΔE_1 [e]/V	E_{pa1} [b]/V	E_{pc1} [c]/V	$E^{0'}{}_1$ [d]/V	ΔE_1 [e]/V
10	-0.0558	-0.0998	-0.100	0.044	-0.0571	-0.0688	-0.069	0.012
20	-0.0455	-0.0957	-0.096	0.050	-0.0456	-0.0688	-0.069	0.023
30	-0.0412	-0.0935	-0.094	0.052	-0.0456	-0.0688	-0.069	0.023
40	-0.0371	-0.0935	-0.094	0.056	-0.0456	-0.0688	-0.069	0.023
50	-0.035	-0.0935	-0.094	0.059	-0.0408	-0.0688	-0.069	0.028
60	-0.0287	-0.0976	-0.098	0.069	-0.0387	-0.0688	-0.069	0.030
70	-0.0225	-0.0976	-0.098	0.075	-0.0387	-0.0688	-0.069	0.030
80	-0.0203	-0.1019	-0.102	0.082	-0.0363	-0.0688	-0.069	0.033
90	-0.0182	-0.1019	-0.102	0.084	-0.0363	-0.0733	-0.073	0.037
100	-0.0164	-0.1032	-0.103	0.087	-0.0363	-0.0733	-0.073	0.037
Average			-0.098	0.066			-0.070	0.028
v [a]/mV s^{-1}	E_{pa2} [b]/V	E_{pc2} [c]/V	$E^{0'}{}_2$ [d]/V	ΔE_2 [e]/V	E_{pa2} [b]/V	E_{pc2} [c]/V	$E^{0'}{}_2$ [d]/V	ΔE_2 [e]/V
10	0.6174	0.5933	0.593	0.024	0.6305	0.6174	0.617	0.013
20	0.6184	0.5912	0.591	0.027	0.6305	0.6174	0.617	0.013
30	0.6205	0.5902	0.590	0.030	0.6274	0.6174	0.617	0.010
40	0.6215	0.5881	0.588	0.033	0.6265	0.6152	0.615	0.011
50	0.6236	0.586	0.586	0.038	0.6274	0.6174	0.617	0.010
60	0.6247	0.5839	0.584	0.041	0.6289	0.6193	0.619	0.010
70	0.6268	0.5818	0.582	0.045	0.6289	0.6193	0.619	0.010
80	0.6278	0.5797	0.580	0.048	0.6314	0.6193	0.619	0.012
90	0.6288	0.5777	0.578	0.051	0.63147	0.6214	0.621	0.010
100	0.631	0.5755	0.576	0.056	0.632	0.6214	0.621	0.011
Average			0.585	0.039			0.619	0.011

v [a]/mV s^{-1}	E_{pa3} [b]/V	E_{pc3} [c]/V	$E^{0'}{}_3$ [d]/V	ΔE_3 [e]/V	E_{pa3} [b]/V	E_{pc3} [c]/V	$E^{0'}{}_3$ [d]/V	ΔE_3 [e]/V
10	0.9414	0.8808	0.881	0.061	0.9289	0.9162	0.916	0.013
20	0.9467	0.8704	0.870	0.076	0.9414	0.9144	0.914	0.027
30	0.9529	0.862	0.862	0.091	0.9454	0.9121	0.912	0.033
40	0.9581	0.8588	0.859	0.099	0.956	0.8996	0.900	0.056
50	0.9623	0.8526	0.853	0.110	0.9622	0.8934	0.893	0.069
60	0.9654	0.8484	0.848	0.117	0.9622	0.8912	0.891	0.071
70	0.9685	0.8411	0.841	0.127	0.9622	0.889	0.889	0.073
80	0.9727	0.8369	0.837	0.136	0.9622	0.885	0.885	0.077
90	0.9769	0.8296	0.830	0.147	0.9622	0.8806	0.881	0.082
100	0.98	0.8233	0.823	0.157	0.9622	0.8766	0.877	0.086
Average			0.850	0.112			0.896	0.059
v [a]/mV s^{-1}	E_{pa4} [b]/V	E_{pc4} [c]/V	$E^{0'}{}_4$ [d]/V	ΔE_4 [e]/V	E_{pa4} [b]/V	E_{pc4} [c]/V	$E^{0'}{}_4$ [d]/V	ΔE_4 [e]/V
10	1.1211	1.0292	1.029	0.092	1.1275	1.0787	1.079	0.049
20	1.1385	1.01202	1.012	0.126	1.1344	1.0603	1.060	0.074
30	1.1295	0.9956	0.996	0.134	1.1368	1.0461	1.046	0.091
40	1.1274	0.981	0.981	0.146	1.1368	1.0371	1.037	0.100
50	1.1252	0.979	0.979	0.146	1.1392	1.0323	1.032	0.107
60	1.1211	0.9706	0.971	0.151	1.1392	1.0229	1.023	0.116
70	1.1211	0.9644	0.964	0.157	1.1392	1.016	1.016	0.123
80	1.1211	0.9601	0.960	0.161	1.1392	1.0115	1.012	0.128
90	1.1211	0.956	0.956	0.165	1.1413	1.0067	1.007	0.135
100	1.1211	0.9521	0.952	0.169	1.1413	1.0067	1.007	0.135
Average			0.980	0.145			1.032	0.106

[a] v: scan rate in mVs^{-1}.
[b] E_{pai}: anodic peak potential of redox couple i, i = 1-4.
[c] E_{pci}: cathodic peak potential of redox couple i, i = 1-4.
[d] $E^{0'}{}_i$: formal potential of redox couple i, i = 1-4.
[e] ΔE_i: peak-to-peak separation of redox couple i, i = 1-4.

Fig. 1B & C showed the cyclic voltammograms of RuHCF/GCE and MWCNT-RuHCF/GCE examined in pH 1.5 with different scan rate. In this test, both of these modified electrodes exhibited four redox couples. The redox peaks were measured as Table 1. By the result, it's obvious to see that the difference between RuHCF and MWCN-RuHCF in the average formal potential ($E^{0'}$) and the average peak-to-peak separation (ΔE_p). The redox couples were found at $E^{0'}{}_1$ = -0.098 V, $E^{0'}{}_2$ = +0.585 V, $E^{0'}{}_3$ = +0.85 V, and $E^{0'}{}_4$ = +0.98 V for RuHCF redox couples. As compared to MWCNT-RuHCF, four redox couples were $E^{0'}{}_1$ = -0.07 V, $E^{0'}{}_2$ = +0.619 V, $E^{0'}{}_3$ = +0.896 V, and $E^{0'}{}_4$ = +1.032 V. It shows positive-potential shift when RuHCF modified with functionalized MWCNT. This might be due to the mixed-valent RuHCF attracted by partial negative-charged carboxylic group to increase the positive potential of redox peaks. When compared the ΔE_p, the MWCNT-RuHCF exhibits the small value to show the more close anodic and cathodic peaks. It means the electron transfer is very fast in MWCNT-RuHCF redox processes and proves the transfer enhanced by MWCNT. This also means that the MWCNT-RuHCF composite is more electroactive and reversible in the electrochemical system.

From the estimation of peak currents, both anodic and cathodic peak currents are also directly proportional to scan rate up to 100 mV s^{-1} (insets of Fig. 1B & C) as expected for surface-confined

process. This also means that this process is diffusion-less controlled and stable in the electrochemical system.

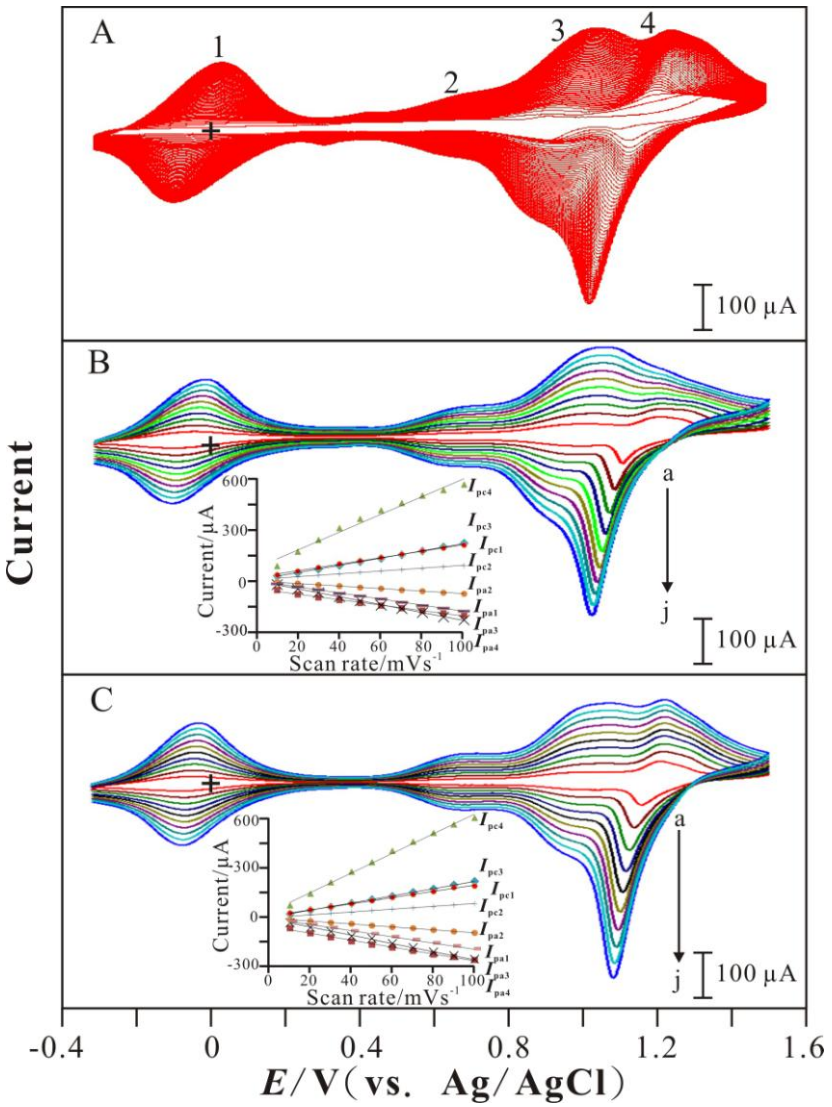

Figure 1. (A) Cyclic voltammograms of RuHCF deposition using GCE in 0.1 M KNO_3 + HNO_3 (pH 1.5) containing 5×10^{-3} M $Ru(NO_3)_3$ and 5×10^{-3} M $K_3Fe(CN)_6$, scan rate = 100 mV s^{-1}; Cyclic voltammograms of (B) RuHCF/GCE and (C) MWCNT-RuHCF/GCE examined in 0.1 M KNO_3 + HNO_3 (pH 1.5) with various scan rates of (a) 10, (b) 20, (c) 30, (d) 40, (e) 50,

The observation of well-defined and persistent cyclic voltammetric peaks indicates that the RuHCF/GCE and MWCNT-RuHCF/GCE exhibit electrochemical response characteristics of redox species confined on the electrode. The linear regressing equations of peak currents (I_{pa} & I_{pc}) and scan rate (v) can be expressed as follows:

At RuHCF/GCE:

$I_{pa1}(\mu A) = -1.83v(mV\ s^{-1}) - 1.66\ (R^2 = 0.9995)$ (5)

$I_{pc1}(\mu A) = 1.87v(mV\ s^{-1}) + 15.89\ (R^2 = 0.9985)$ (6)

$I_{pa2}(\mu A) = -0.77v(mV\ s^{-1}) - 3.20\ (R^2 = 0.9982)$ (7)

$I_{pc2}(\mu A) = 0.84v(mV\ s^{-1}) + 4.10\ (R^2 = 0.9985)$ (8)

$I_{pa3}(\mu A) = -2.36v(mV\ s^{-1}) - 3.60\ (R^2 = 0.9991)$ (9)

$I_{pc3}(\mu A) = 2.18v(mV\ s^{-1}) + 2.18\ (R^2 = 0.9994)$ (10)

$I_{pa4}(\mu A) = -1.64v(mV\ s^{-1}) - 49.16\ (R^2 = 0.9956)$ (11)

$I_{pc4}(\mu A) = 5.32v(mV\ s^{-1}) + 73.84\ (R^2 = 0.9768)$ (12)

At MWCNT-RuHCF/GCE:

$I_{pa1}(\mu A) = -1.84v(mV\ s^{-1}) - 2.16\ (R^2 = 0.9998)$ (13)

$I_{pc1}(\mu A) = 1.96v\ (mV\ s^{-1}) + 12.70\ (R^2 = 0.9981)$ (14)

$I_{pa2}(\mu A) = -0.88v\ (mV\ s^{-1}) - 0.37\ (R^2 = 0.9990)$ (15)

$I_{pc2}(\mu A) = 0.86v\ (mV\ s^{-1}) + 2.23\ (R^2 = 0.9992)$ (16)

$I_{pa3}(\mu A) = -2.46v\ (mV\ s^{-1}) - 4.80\ (R^2 = 0.9985)$ (17)

$I_{pc3}(\mu A) = 2.18v\ (mV\ s^{-1}) + 3.91\ (R^2 = 0.9997)$ (18)

$I_{pa4}(\mu A) = -2.08v\ (mV\ s^{-1}) - 49.67\ (R^2 = 0.9937)$ (19)

$I_{pc4}(\mu A) = 5.93v\ (mV\ s^{-1}) + 35.49\ (R^2 = 0.9978)$ (20)

It shows good linearity in the regressing equations. It is also noticed that the absolute values of slope are almost larger in redox peaks than that of RuHCF without MWCNT. This means that the peak current is enhanced by MWCNT. Considering the occupation of electroactive species, we have estimated, the apparent surface coverage (Γ), by using Eq. (21):

$$I_p = n^2F^2vA\Gamma/4RT \quad (21)$$

where, I_p is the peak current of the MWCNT-RuHCF composite electrode; n is the number of electron transfer; F is Faraday constant (96485 C mol^{-1}); v is the scan rate (mV s^{-1}); A is the area of the electrode surface (0.07 cm^2); R is gas constant (8.314 J mol^{-1} K^{-1}); and T is the room temperature (298.15 K). In the present case, the calculated surface coverage (Γ) was 2.5×10^{-8} mol cm^{-2} assuming a one-electron process for RuHCF. By comparison between RuHCF and MWCNT-RuHCF, the Γ of MWCNT is calculated in 6.6×10^{-9} mol cm^{-2}.

3.2. SEM analysis of RuHCF and MWCNT hybrid film

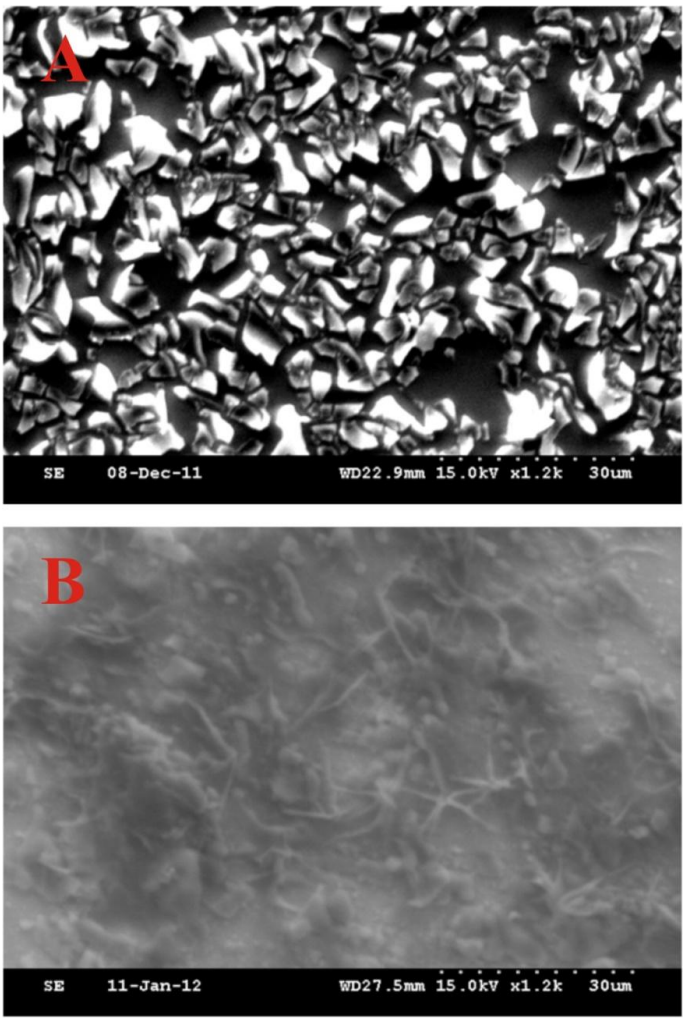

Figure 2. SEM images of (A) RuHCF/ITO and (B) MWCNT-RuHCF/ITO.

SEM was utilized to image the morphology of the active surface of the electrodeposited RuHCF films with/without MWCNT as shown in Fig. 2. Fig. 2A shows the RuHCF image which exhibits the rough irregular shape due to the mixed-valent RuHCF composite. When this composite is further adhered with MWCNT, it shows smooth surface and fiber-like shape as shown in Fig. 2B. The fiber-like structure may be the result of MWCNT aggregation. This might mean that the rough RuHCF composite can be filled up with MWCNT to make more compact structure.

3.3. Electrocatalytic properties of RuHCF and MWCNT hybrid film

The RuHCF with/without MWCNT were examined for the electrocatalytic oxidation of alcohols and sulfides, and the electrocatalytic reduction of H_2O_2 by cyclic voltammetry. The alcohols and sulfides including methanol, ethanol, propanol, isopropanol, L-cysteine, and thiosulfate were individually taken for electrocatalytic oxidation.

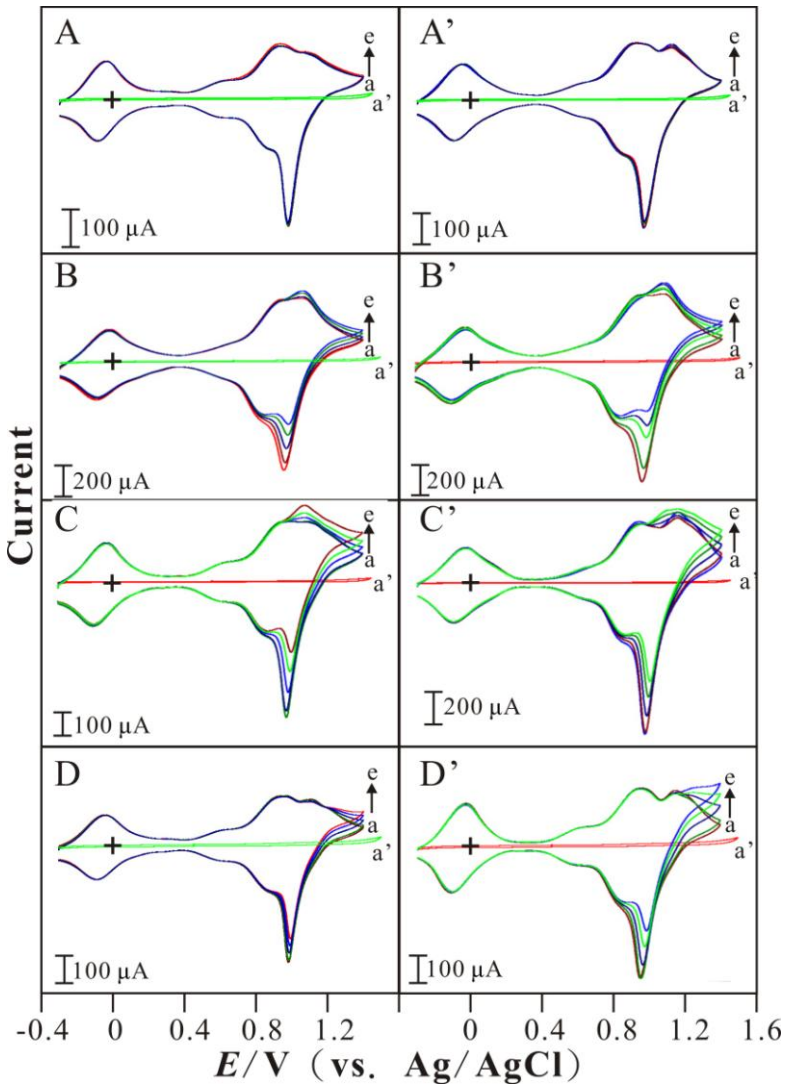

Figure 3. Cyclic voltammograms of RuHCF/GCE examined in 0.1 M KNO_3 + HNO_3 (pH 1.5) with various reactants of (A) methanol, (B) ethanol, (C) propanol, (D) isopropanol in the concentration of (a) 0, (b) 1×10^{-3}, (c) 5×10^{-3}, (d) 1×10^{-2}, (e) 1.5×10^{-2} M, respectively. (A')—(D') are the relative cases using MWCNT-RuHCF/GCE. Scan rate = 0.1 Vs^{-1}.

Fig. 3A & A' show the cyclic voltammograms for (A) RuHCF/GCE and (A') MWCNT-RuHCF/GCE examined in nitric solution (pH 1.5) with different methanol concentration. In both cases, no current increased in the redox peaks as compared with the blank signal. It means that both

composites are not able to show the electrocatalytic activity to methanol even in the presence of MWCNT.

Fig. 3B & B' show the cyclic voltammograms for (B) RuHCF/GCE and (B') MWCNT-RuHCF/GCE examined in nitric solution (pH 1.5) with different ethanol concentration. In both cases, one electrocatalytic oxidation peak was observed at about +1.05 V. The oxidation current increases as the increase of ethanol concentration. One can know that the hybrid composite lowers the over-potential for ethanol oxidation as compared to bare electrode. The electrocatalytic reaction can be expressed as follow:

$$Ru^{IV}HCF/GCE + CH_3CH_2OH \rightarrow Ru^{III}HCF/GCE + CH_3CHO + H_2O \qquad (22)$$

Fig. 3C & C' show the cyclic voltammograms for (C) RuHCF/GCE and (C') MWCNT-RuHCF/GCE examined in nitric solution (pH 1.5) with different propanol concentration. In both cases, one electrocatalytic oxidation peak was observed at about +1.05 V. The oxidation current increases as the increase of propanol concentration. One can know that the hybrid composite lowers the over-potential for propanol oxidation as compared to bare electrode. The electrocatalytic reaction can be expressed as follow:

$$Ru^{IV}HCF/GCE + CH_3CH_2CH_2OH \rightarrow Ru^{III}HCF/GCE + CH_3CH_2CHO + H_2O \qquad (23)$$

Fig. 3D & D' show the cyclic voltammograms for (D) RuHCF/GCE and (D') MWCNT-RuHCF/GCE examined in nitric solution (pH 1.5) with different isopropanol concentration. In both cases, one electrocatalytic oxidation peak was observed at about +1.25 V. The oxidation current increases as the increase of isopropanol concentration. One can know that the hybrid composite lowers the over-potential for isopropanol oxidation as compared to bare electrode. The electrocatalytic reaction can be expressed as follow:

$$Ru^{IV}HCF/GCE + (CH_3)_2CHOH \rightarrow Ru^{III}HCF/GCE + (CH_3)_2CO + H_2O \qquad (24)$$

Fig. 4 shows the voltammetric response for electrocatalytic oxidation of L-cysteine and thisulfate by RuHCF and MWCNT-RuHCF, respectively. Particularly, three electrocatalytic oxidation peaks are individually recognized at +0.36 V, +0.95 V, +1.16 V, and +0.58 V, +0.95 V, +1.12 V for L-cysteine and thiosulfate, respectively. It means that both RuHCF and MWCNT-RuHCF composite are electroactive to these species. By estimation of current response, the MWCN-RuHCF also exhibits much higher current response than that of RuHCF. That means the MWCNT only enhances the electrocatalytic current instead of electro-oxidation potential in this case. The electrocatalytic reaction oxidized L-cysteine (CySH) to L-cystine (CySSCy) can be expressed as follow:

$$2CySH \rightarrow CySSCy + 2H^+ + 2e^- \qquad (25)$$

And, the electro catalytic oxidation of thiosulphate can be represented as follow:

$$2S_2O_3^{2-} \rightarrow S_4O_6^{2-} + 2e^- \quad (26)$$

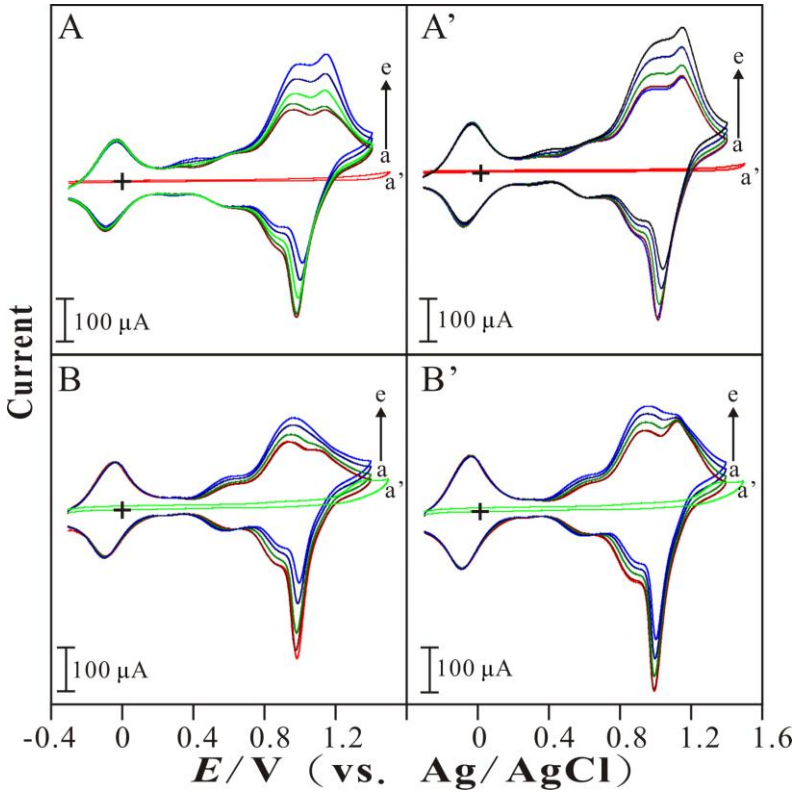

Figure 4. Cyclic voltammograms of RuHCF/GCE examined in 0.1 M KNO_3 + HNO_3 (pH 1.5) with various reactants of (A) [L-cysteine] = (a) 0, (b) 1×10^{-4}, (c) 5×10^{-4}, (d) 1×10^{-3}, (e) 1.5×10^{-3} M; and (B) [$Na_2S_2O_3$] = (a) 0, (b) 1×10^{-4}, (c) 5×10^{-4}, (d) 1×10^{-3}, (e) 1.5×10^{-3} M, respectively. (A') & (B') are the relative cases using MWCNT-RuHCF/GCE. Scan rate = 0.1 Vs^{-1}.

The electrocatalytic reaction of H_2O_2 was studied with different initial potential ($E_{initial}$) in the same potential range as shown in Fig. 5. It was done in positive scan ($E_{initial}$ = -0.3 V) and negative scan ($E_{initial}$ = +1.4 V) to have the voltammetric response of RuHCF/GCE as Fig. 5A & B. These two cases were found not only current increased at oxidation peaks of +1.05 V and +1.18 V but also at reduction peak at -0.07 V. This means that the voltammetric peaks will not vary by different $E_{initial}$. The symmetric experiments were also done by MWCNT-RuHCF (as shown in Fig. 5A' & B') with similar reaction peaks but higher current response. Both RuHCF and MWCNT-RuHCF have electroactivity to oxidize and reduce H_2O_2 in the same solution. It indicates that the activation energy of H_2O_2 is only dependent on modifiers on electrode surface. Although it exhibits almost the same reaction peaks, the electrocatalytic reduction current is larger at E_{pc} = -0.07 V. This indicates that the H_2O_2 is oxidized firstly to form oxygen and the impermanent O_2 (adsorbed on electrode surface) is further reduced to H_2O or H_2O_2 in negative scan. The reaction formula can be expressed as follows:

$$2H_2O_2 \rightarrow O_2 + 2H_2O \quad (27)$$

$$O_2 + 2H_2O \rightarrow 2H_2O_2 \quad (28)$$

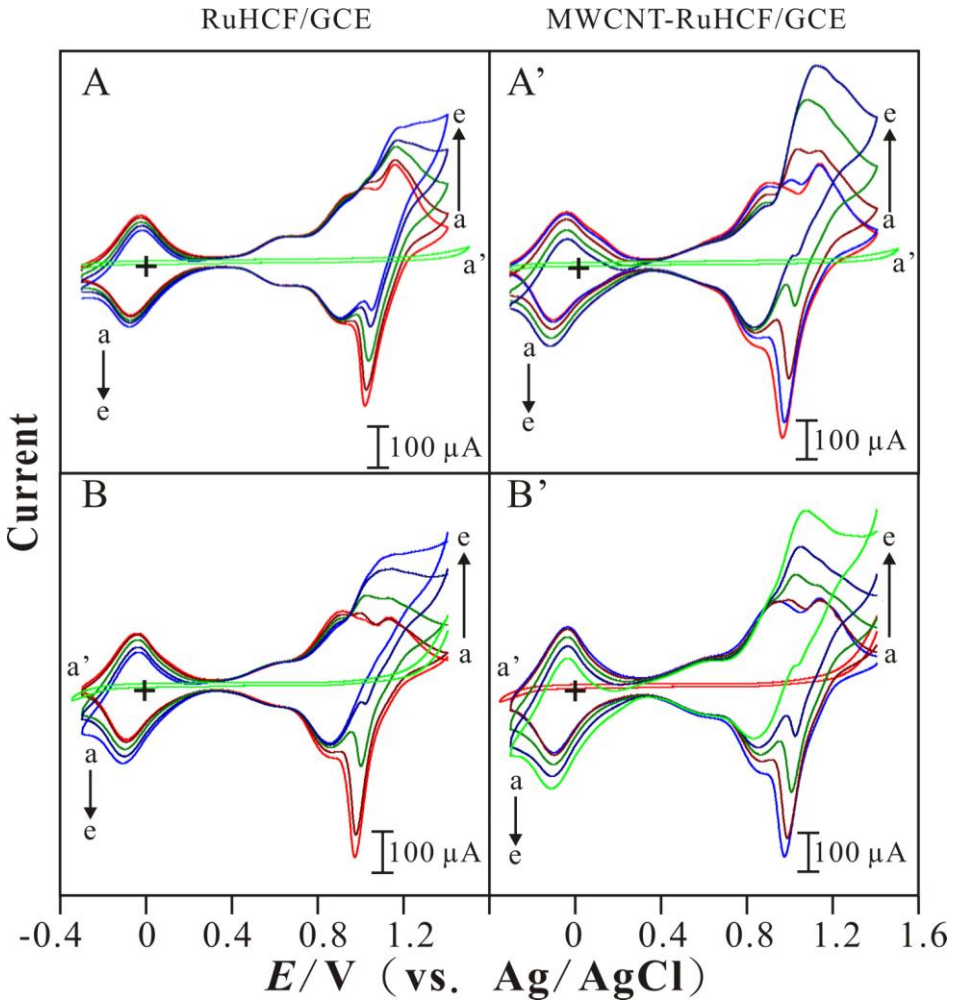

Figure 5. Cyclic voltammograms of RuHCF/GCE examined in 0.1 M KNO_3 + HNO_3 (pH 1.5) with various concentration of $[H_2O_2]$ = (a) 0, (b) 1×10^{-3}, (c) 5×10^{-3}, (d) 1×10^{-2}, (e) 1.5×10^{-2} M, respectively. Scan rate = 0.1 Vs^{-1}. (A) & (B) are the voltammograms with positive and negative scan, respectively. (A') & (B') are the relative cases using MWCNT-RuHCF/GCE.

Hence we can see the higher anodic peak current is found at E_{pa} = +1.05 V and E_{pa} = +1.18 V in the negative scan. One can conclude that the current response will vary due to different oxidation-reduction procedures. Moreover, the current enhancement to have higher current response can be achieved by using MWCNT.

By estimation and comparison of the electrocatalytic oxidation/reduction current between RuHCF and MWCNT-RuHCF in above cases, it is noticed that the MWCNT-RuHCF shows several times than that in the absence of MWCNT. One can know that the electrocatalytic oxidation of ethanol, propanol, isopropanol, and the electrocatalytic oxidation/reduction of H_2O_2 can be performed by RuHCF and further enhanced by MWCNT. The reasons to explain this behavior might be the faster electron-transfer rate due to the modification by MWCNT-RuHCF hybrid composite and its action as a good electrocatalyst. For quantification, this electrode was further used to study the determination of ethanol, propanol, isopropanol, and H_2O_2 by amperometry.

3.4. Amperometric response of ethanol, propanol, isopropanol, and H_2O_2 at MWCNT-RuHCF hybrid film modified electrode

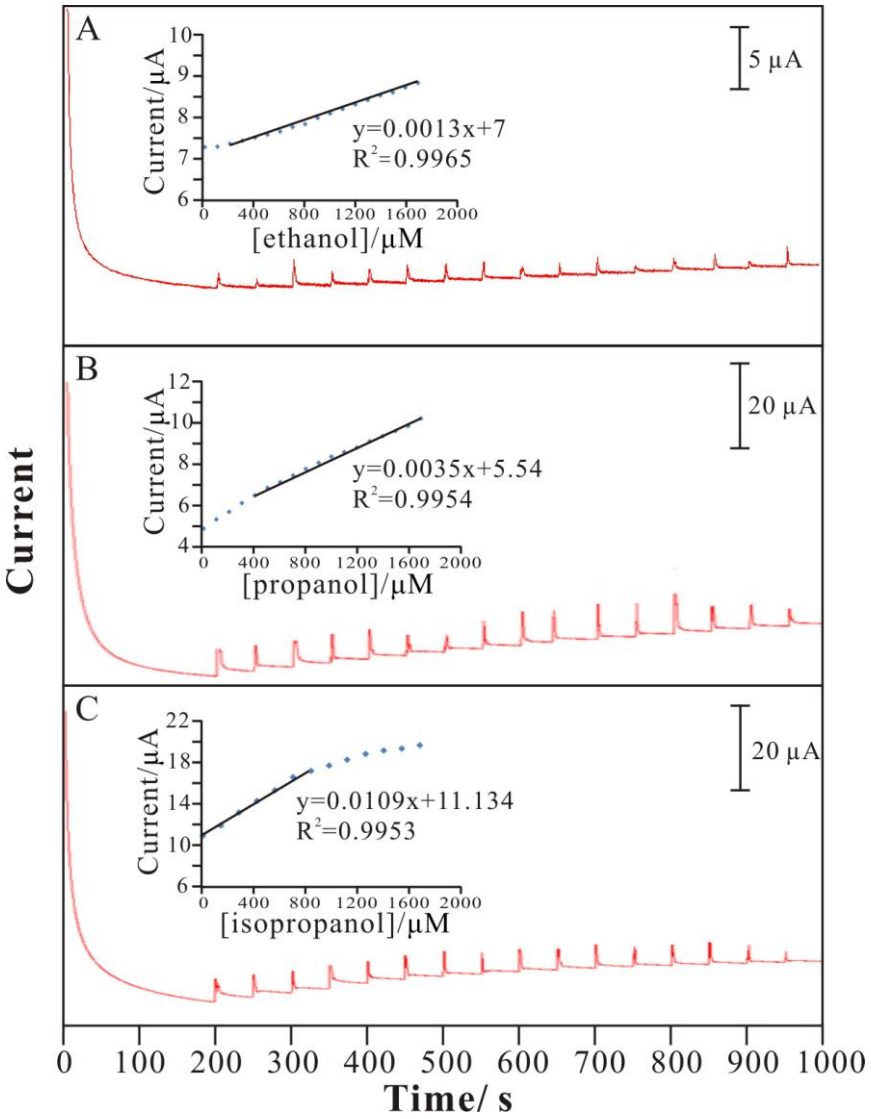

Figure 6. Amperometric responses of sequential additions of (A) ethanol (10^{-4} M per time), (B) propanol, and (C) isopropanol tested by MWCNT-RuHCF/GCE in 0.1 M PBS (pH 7) solution, rotation speed = 1000 rpm. The working potential applied at $E_{app.}$ = +1.05 V, +1.15 V, and +1.23 V, respectively. Insets: the plots of current response vs. concentration.

Fig. 6 shows the amperometric response of MWCNT-RuHCF/GCE to ethanol, propanol, and isopropanol by amperometry. Amperometric measurements were individually applied at a constant potential at +1.05 V, +1.15 V and +1.23 V, taken with different concentrations of these species in nitric solution (pH 1.5), clearly demonstrate that MWCNT-RuHCF/GCE works well as an ethanol, propanol, and isopropanol amperometric sensor. The sensor response time was short, reaching 100% (steady-state current) of its maximum response less than 1 s, which also demonstrates the high stability of the signal as a function of time. Furthermore, the proposed sensor showed a linear response ranging of 2×10^{-4}–1.7×10^{-3} M, 4×10^{-4}–1.7×10^{-3} M, and 0–8×10^{-4} M (insets of Fig. 6), with sensitivity of 4548.4 μA M^{-1} cm^{-2}, 12544.6 μA M^{-1} cm^{-2}, and 38543.1 μA M^{-1} cm^{-2} for ethanol, propanol, and

isopropanol, respectively. The linear regressing equation between peak current and concentration ($C_{ethanol}$, $C_{propanol}$, $C_{isopropanol}$) can be expressed as follows:

$$I_p(\mu A) = 0.0013C_{ethanol}(\mu mol\ l^{-1}) + 7\ (R^2 = 0.9965) \quad (29)$$

$$I_p(\mu A) = 0.0035C_{propanol}(\mu mol\ l^{-1}) + 5.54\ (R^2 = 0.9954) \quad (30)$$

$$I_p(\mu A) = 0.0109C_{isopropanol}(\mu mol\ l^{-1}) + 11.13\ (R^2 = 0.9953) \quad (31)$$

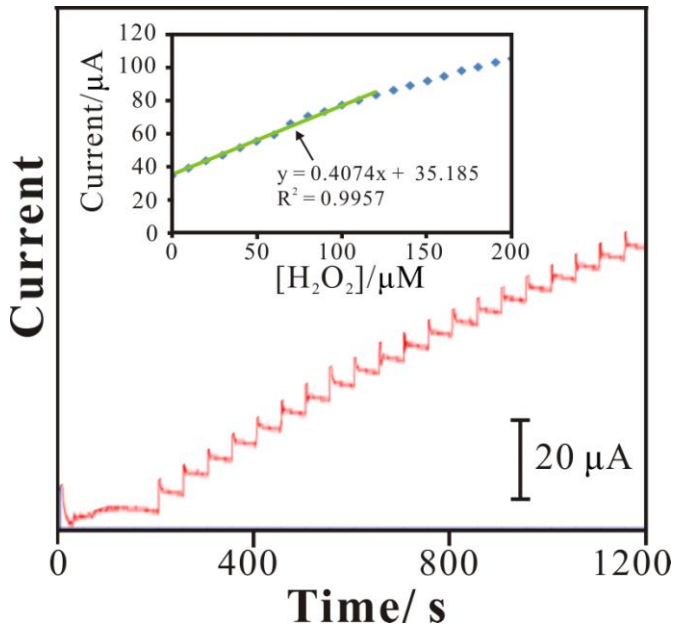

Figure 7. Amperometric responses of sequential additions of H_2O_2 (10^{-4} M per time) tested by MWCNT-RuHCF/GCE in 0.1 M PBS (pH 7) solution, rotation speed = 1000 rpm, $E_{app.}$ = -0.1 V (Inset: the plot of current response vs. H_2O_2 concentration).

Fig. 7 shows the amperometric response of MWCNT-RuHCF/GCE to H_2O_2 by amperometry. Amperometric measurements were applied at a constant potential at -0.1 V, taken with different concentrations of H_2O_2 in nitric solution (pH 1.5). It showed a linear response range of 0–1.2×10^{-4} M (inset of Fig. 7), with sensitivity of 123.2 μA mM^{-1} cm^{-2}. The linear regressing equation between peak current and concentration (C_{H2O2}) can be expressed as follow:

$$I_p(\mu A) = 0.4074C_{H2O2}(\mu mol\ l^{-1}) + 35.185\ (R^2 = 0.9957) \quad (32)$$

By the results, this composite modified electrode exhibits competitive performance for ethanol sensing when compared to some related topics [63,64]. This also indicates that both of voltammetry and amperometry can help to determine the target species including alcohols, sulfides and hydrogen peroxide.

3.5. Stability study of MWCNT-RuHCF hybrid film

The stability of the MWCNT-RuHCF redox couples were checked by performing successive cyclic voltammograms in a potential range of -0.3 to +1.4 V and in the presence of 0.5 mM ethanol and H_2O_2, respectively. After 100 scans and 50 ethanol and H_2O_2 determinations, no significant change was observed in the voltammetric response, indicating that the MWCNT-RuHCF/GCE modified electrode is very stable.

4. CONCLUSIONS

Here we report a method to form a multifunctional sensor of ethanol, propanol, isopropanol, and H_2O_2 based on MWCNT-RuHCF hybrid composite. It shows good electrocatalytic oxidation and reduction with lower over-potential and higher current response as compared with bare electrode and RuHCF. Amperometric response of MWCNT-RuHCF/GCE is linearly dependent on ethanol, propanol, isopropanol, and H_2O_2 concentration. The proposed film also shows good electrocatalytic oxidation for L-cysteine and thiosulfate, respectively. As the results, the proposed method has advantages of multifunction, simple method, low over-potential, and high current response. It has potential to develop a multifunctional sensor.

ACKNOWLEDGEMENTS
This work was supported by the National Science Council of Taiwan (ROC).

References

1. Y. Liu, L. Xu, *Sensors* 7 (2007) 2446.
2. A. Abbaspour, A. Ghaffarinejad, *Electrochim. Acta* 53 (2008) 6643.
3. L. Shi, T. Wu, P. He, D. Li, Ch. Sun, J. Li, *Electroanalysis* 17 (2005) 2190.
4. S. Ayrault, B. Jimenez, E. Granier, E. Fedoroff, M.D.J. Jones, C. Loos-Neskovic, *J. Solid State Chem.* 141 (1998) 475.
5. S.M. Chen, *J. Electroanal. Chem.* 417 (1996) 145.
6. S.M. Chen, K.T. Peng, *J. Electroanal. Chem.* 547 (2003) 179.
7. S.M. Chen, *Electrochim. Acta* 43 (1998) 3359.
8. S.M. Chen, *J. Electroanal. Chem.* 521 (2002) 29.
9. B. Devadas, M. Rajkumar, S.M. Chen, R. Saraswathi, *Int. J. Electrochem. Sci.* 7 (2012) 3339.
10. T.H. Tsai, T.W. Chen, S.M. Chen, R. Sarawathi, *Russ. J. Electrochem.* 48 (2012) 291.
11. S.M. Chen, C.H. Wang, K.C. Lin, *Int. J. Electrochem. Sci.* 7 (2012) 405.
12. A.P. Periasamy, J.X. Wei , S.M. Chen, *Int. J. Electrochem. Sci.* 6 (2011) 4422.
13. T.H. Tsai, T.W. Chen, S.M. Chen, *Int. J. Electrochem. Sci.* 6 (2011) 4628.
14. T.H. Tsai, T.W. Chen, S.M. Chen, K.C. Lin, *Int. J. Electrochem. Sci.* 6 (2011) 2058.
15. Q. Xu, S. Zhang, W. Zhang, L.T. Jin, K. Tanaka, H. Haraguchi, A. Itoh, *Fresenius J. Anal. Chem.* 367 (2000) 241.
16. J. Wang, X.J. Zhang, L. Chen, *Electroanalysis* 16 (2000) 1277.
17. A. Salimi, K. Abdi, *Talanta* 63 (2004) 475.

18. C.X. Cai, K.H. Xue, S.M. Xu, *J. Electroanal. Chem.* 486 (2000) 111.
19. M.H. Pournaghi-Azar, H. Razmi-Nerbin, B. Hafezi, *Electroanalysis* 14 (2002) 206.
20. J.W. Mo, B. Ogorevc, X.J. Zhang, B. Pihlar, *Electroanalysis* 12 (2000) 48.
21. W.Y. Tao, D.W. Pan, Y.J. Liu, L.H. Nie, S.Z. Yao, *Anal. Biochem.* 338 (2005) 332.
22. M.H. Pournaghi-Azar, H. Dastangoo, *J. Electroanal. Chem.* 523 (2002) 26.
23. R.O. Lezna, R. Romagnoli, N.R. de Tacconi, K. Rajeshwar, *J. Electroanal. Chem.* 544 (2003) 101.
24. E. Cziro'k, J. Ba'cskai, P.J. Kulesza, G. Inzelt, A. Wolkiewicz, K. Miecznikowski, M.A. Malik, *J. Electroanal. Chem.* 405 (1996) 205.
25. Y. Wang, G.Y. Zhu, E.K. Wang, *J. Electroanal. Chem.* 430 (1997) 127.
26. A. Ro'ka, I. Varga, G. Inzelt, *Electrochim. Acta* 51 (2006) 6243.
27. K. Kasem, F.R. Steldt, T.J. Miller, A.N. Zimmerman, *Micropor. Mesopor. Mater.* 66 (2003) 133.
28. S.M. Chen, M.F. Lu, K.C. Lin, *J. Electroanal. Chem.* 579 (2005) 163.
29. Z.Y. Xun, C.X. Cai, W. Xing, T.H. Lu, *J. Electroanal. Chem.* 545 (2003) 19.
30. J. Bacskai, K. Martinusz, E. Czirok, G. Inzelt, P.J. Kulesza, M.A. Malik, *J. Electroanal. Chem.* 385 (1995) 241.
31. A. Eftekhari, *J. Electroanal. Chem.* 537 (2002) 59.
32. M.H. Pournaghi-Azar, H. Nahalparvari, *Electrochim. Acta* 50 (2005) 2107.
33. J. Zheng, Q. Sheng, L. Li, Y. Shen, *J. Electroanal. Chem.* 611 (2007) 155.
34. M.Z. Jacobson, W.G. Colella, D.M. Golden, *Science* 308 (2005) 1901.
35. K.V. Kordesch, G.R. Simader, *Chem. Rev.* 95 (1995) 191.
36. C. Binachini, P.K. Shen, *Chem. Rev.* 109 (2009) 4183.
37. R.F. Service, *Science* 296 (2002) 1222.
38. A.K. Shukla, R.K. Raman, *Annu. Rev. Mater. Res.* 33 (2003) 155.
39. K. Kleiner, *Nature* 441 (2006) 1046.
40. S. Liao, K.A. Holmes, H. Tsaprailis, V.I. Birss, *J. Am. Chem. Soc.* 128 (2006) 3504.
41. S. Wasmus, A. Kuver, *J. Electroanal. Chem.* 461 (1999) 14.
42. M.L. Hung, D.M. Stanbury, *Inorg. Chem.* 44 (2005) 3541.
43. T. Inoue, J.R. Kirchhoff, *Anal. Chem.* 72 (2000) 5755.
44. S. Jahandideh, S. Hoseini, M. Jahandideh, A. Hoseini, A.S. Yazdi, *Comput. Biol. Med.* 39 (2009) 332.
45. H.R.J. Hosseini, M. Aminlari, M.R. Khalili, *Iran. Red Crescent Med. J.* 10 (2008) 281.
46. W. Droge, H.P. Eck, H. Gmunder, S. Mihm, *Am. J. Med.* 91 (1991) 140S.
47. H. Heli, M. Hajjizadeh, A. Jabbari, A.A. Moosavi-Movahedi, *Anal. Biochem.* 388 (2009) 81.
48. G. Herzog, D.W.M. Arrigan, *Analyst* 132 (2007) 615.
49. I. Molnar-Perl, *J. Chromatogr. A* 987 (2003) 291.
50. J. Lock, J. Davis, *Trends Anal. Chem.* 21 (2002) 807.
51. G.S. Owens, W.R. LaCourse, *J. Chromatogr. B* 695 (1997) 15.
52. P.J. Vandeberg, D.C. Johnson, *Anal. Chem.* 65 (1993) 2713.
53. T. Inoue, J.R. Kirchhoff, *Anal. Chem.* 74 (2002) 1349.
54. D. Mimica, F. Bedioui, J.H. Zagal, *Electrochim. Acta* 48 (2002) 323.
55. K.C. Lin, T.H. Tsai, S.M. Chen, *Biosens. Bioelectron.* 26 (2010) 608.
56. B. Unnikrishnan, S. Palanisamy, S.M. Chen, *Biosens. Bioelectron.* 39 (2013) 70.
57. A.P. Periasamy, Y.H. Ho, S.M. Chen, *Biosens. Bioelectron.* 29 (2011) 151.
58. M. Zhou, Y.M. Zhai, S.J. Dong, *Anal. Chem.* 81 (2009) 5603.
59. O.S. Wolfbeis, A. Durkop, M. Wu, Z.H. Lin, *Angew. Chem. Int. Ed.* 41 (2002) 4495.
60. S.Q. Liu, H. Li, W.H. Sun, X.M. Wang, Z.G. Chen, J.J. Xu, H.X. Ju, H.Y. Chen, *Electrochim. Acta* 56 (2011) 4007.
61. U. Yogeswaran, S. Thiagarajan, S.M. Chen, *Anal. Biochem.* 365 (2007) 122.
62. U. Yogeswaran, S.M. Chen, *Anal. Lett.* 41 (2008) 210.
63. A.S. Adekunle, O.S. Oluwafemi, V. Ncapayi, R.E. Sadiku, J.T. Agee, S.O. Ojo, S.P. Songca, *Int. J.*

Electrochem. Sci. 7 (2012) 2695.
64. F. Salimi , M. Negahdary, G. Mazaheri, H. Akbari-dastjerdi, Y. Ghanbari-kakavandi, S. Javadi, S.H. Inanloo, M. Mirhashemi-route, M.H. Shokoohnia, A. Sayad, *Int. J. Electrochem. Sci.* 7 (2012) 7225.